



CHORUS

This is the accepted manuscript made available via CHORUS. The article has been published as:

Dimensional crossover in the electrical and magnetic properties of the layered LaSb_2 superconductor under pressure: The role of phase fluctuations

S. Guo, D. P. Young, P. W. Adams, X. S. Wu, Julia Y. Chan, G. T. McCandless, and J. F. DiTusa

Phys. Rev. B **83**, 174520 — Published 31 May 2011

DOI: [10.1103/PhysRevB.83.174520](https://doi.org/10.1103/PhysRevB.83.174520)

Anisotropic superconductivity in layered LaSb₂: the role of phase fluctuations

S. Guo,¹ D.P. Young,¹ P. W. Adams,¹ X. S. Wu,¹ Julia Y. Chan,² G.T. McCandless,² and J.F. DiTusa^{1,*}

¹*Department of Physics and Astronomy, Louisiana State University, Baton Rouge, Louisiana 70803, USA*

²*Department of Chemistry, Louisiana State University, Baton Rouge, Louisiana 70803, USA*

(Dated: March 21, 2011)

We present electrical transport, magnetization, and ac as well as dc magnetic susceptibility measurements of the highly anisotropic compound LaSb₂. Our data display a very broad, anisotropic, transition upon cooling below 2.5 K into a clean superconducting state with a field dependent magnetization that is consistent with type-I behavior. We identify distinct features of 2 dimensionality in both the transport and magnetic properties. Application of hydrostatic pressure induces a 2- to 3-dimensional crossover evidenced by a reduced anisotropy and transition width. The superconducting transition appears phase fluctuation limited at ambient pressure with fluctuations observed for temperatures greater than 8 times the superconducting critical temperature.

PACS numbers: 74.62.Fj, 74.62.-c, 74.40.-n, 74.70.Ad

I. I. INTRODUCTION

Superconductivity in reduced dimensions has intrigued condensed matter physicists for over 40 years. Highly anisotropic materials with superconducting (SC) phases, such as TaS₂ and NbSe₂¹⁻⁶, as well as thin SC metallic films⁷⁻¹⁰ and organic compounds¹¹ were investigated to search for novel properties stemming from dimensionality effects. More recent discoveries of unconventional superconductivity in layered cuprates¹², MgB₂¹³, and iron pnictides¹⁴⁻¹⁷, all possessing anisotropic crystal structures, has highlighted the importance of the layered structure in determining the SC and normal properties of these compounds.

One of the more interesting discoveries in these layered superconductors is the realization that fluctuations in the superconducting phase may play a dominant role in determining the superconducting critical temperature, T_c . The superconducting order parameter has both an amplitude and phase and for nearly all superconducting materials the phase is unimportant in determining T_c . Quasiparticle pairing and long range phase coherence occur essentially simultaneously at T_c . However, as Emery and Kivelson have pointed out, this is likely not to be true under the conditions of low superconducting carrier density and quasi-two-dimensionality. These conditions are realized in the underdoped cuprate superconductors as they are derived by small doping of layered Mott insulating parent compounds^{18,19}. Experiments in these underdoped materials find evidence for pairing well above T_c ,²⁰⁻²² and indicate the importance of phase fluctuations at temperatures, $T \sim T_c$ ¹⁹.

Here we present resistivity, magnetization, and ac susceptibility measurements on the highly layered, low carrier density, SC compound LaSb₂²³⁻²⁵. LaSb₂ has been of interest because of its large, linear in magnetic field, magnetoresistance which is still poorly understood²⁶. Previous transport, photoemission, and optical conductivity investigations reveal LaSb₂ to be a good low carrier density metal with no indications of competing order such as a charge density wave transition^{25,27}. We present evi-

dence that the ambient pressure SC phase, in which only a minority of crystals display a complete Meissner effect at low temperature is characteristic of poorly coupled two dimensional (2D) SC planes. The anisotropy is reduced and the transition is dramatically sharpened as pressure is applied indicating a crossover from a 2D to a more traditional 3D SC phase. Our data demonstrate that the extraordinarily wide, and many times incomplete, SC transition at ambient pressure likely results from 2D phase fluctuations. These phase fluctuations persist for temperatures much lower than the onset temperature for superconductivity, T_{onset} , that is at temperatures an order of magnitude larger than the global SC critical temperature, T_c . This places LaSb₂ among a handful of systems^{9,10,19} exhibiting phase fluctuation limited superconductivity and is unusual in that it displays behavior consistent with clean, type I, superconductivity²⁸.

II. II. EXPERIMENTAL DETAILS

LaSb₂ is a member of the RSb₂ (R=La-Nd, Sm) family of compounds that all form in the orthorhombic, highly layered, SmSb₂ structure^{23,26,29} in which alternating La/Sb layers and 2D rectangular sheets of Sb atoms are stacked along the c-axis. These structural characteristics give rise to the anisotropic physical properties observed in all the compounds in the RSb₂ series^{23,24,26}. A large number of single crystals of LaSb₂ were grown from high purity La and Sb by the metallic flux method. The resulting crystals were large flat, micaceous, plates, which are malleable and easily cleaved. In addition, polycrystalline samples grown in crucibles using a stoichiometric mixture of the constituents had T_{onset} essentially identical to the crystals. The SmSb₂ structure-type with lattice constants of $a = 0.6219(15)$, $b = 0.6278(15)$, and $c = 1.846(5)$ nm with $Z = 8$, was confirmed by single crystal X-ray diffraction. Resistivity, ρ , measurements were performed with currents either in the ab-plane or along the c-axis using standard 4-probe ac techniques at 17 or 27 Hz from $0.05 \leq T \leq 300$ K. Data presented

here are from single crystal samples with residual resistance ratios of 70-90 between 300 and 4 K. Magnetization, M , and susceptibility, χ , were measured with a Quantum Design SQUID magnetometer for $T > 1.75$ K and a dilution refrigerator ac susceptibility probe for $T \geq 50$ mK. These were corrected for demagnetization effects based upon crystal dimensions. Our ac susceptibility measurements were found to be free of Eddy currents effects as our measurements were independent of excitation frequency and amplitude in the range of parameters employed. The susceptibility of several crystals was measured in the SQUID magnetometer with applied hydrostatic pressure, P , of up to 6.5 kbar in a beryllium-copper cell previously described³⁰.

III. EXPERIMENTAL RESULTS

A. Resistivity

Shown in Fig. 1 is the resistivity measured with the current in the ab plane, ρ_{ab} , and along the c -axis, ρ_c , of LaSb_2 as a function of T in zero magnetic field, H . Note that the normal state resistivity is highly anisotropic with $\rho_{ab} = 1.2 \mu\Omega \text{ cm}$ at 4 K and $\rho_c/\rho_{ab} \sim 200$. The ρ_{ab} data suggest a broad SC transition with an onset apparent near $T_{onset} \sim 1.7$ K. This onset temperature varied from sample to sample with crystals having T_{onset} as high as 2.5 K. Nonetheless, a true $\rho = 0$ state is not reached until 0.7 K. In contrast, the T dependence of ρ_c indicates an onset near 1.0 K followed by a $\rho = 0$ state below 0.5 K. Interestingly, the ρ_c curve also shows a small peak for $T < T_{onset}$ similar to what has been reported in $(\text{LaSe})_{1.14}(\text{NbSe}_2)^{31}$ and attributed to a quasiparticle tunneling channel in the interlayer transport.

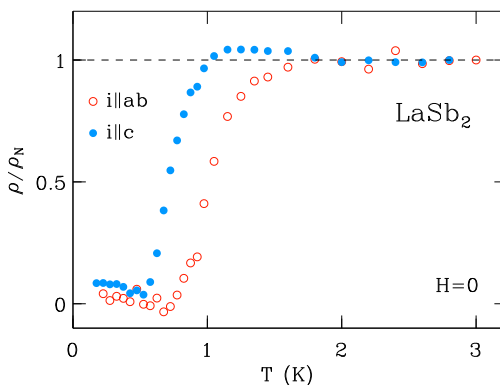


FIG. 1: Resistivity. Resistivity, ρ , divided by the normal state resistivity, ρ_N , vs. temperature, T , for currents along the ab -plane and the c -axis.

All of these features can be suppressed with the application of magnetic fields as demonstrated in Fig. 2 where a compelling difference in ρ_{ab} and ρ_c with H oriented along the ab planes is displayed. We observe that

a field of ~ 500 Oe completely destroys the SC currents along the c -axis while their counterparts in the ab planes remain intact. This demonstrates a relatively poor coupling between the SC condensate residing on neighboring Sb planes.

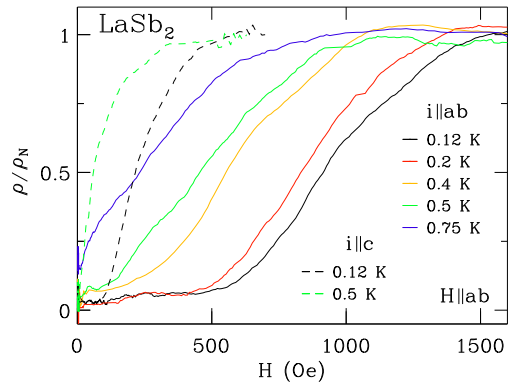


FIG. 2: Field dependence of Resistivity. Resistivity, ρ , divided by the normal state resistivity, ρ_N , ρ/ρ_N vs. magnetic field, H , in the ab plane for currents perpendicular to H in plane and along the c -axis.

B. Magnetic Susceptibility and Magnetization

Similar features are observed in the magnetic response of the SC phase of LaSb_2 , Fig. 3. Because χ and M are representative of the thermodynamic state of this system, the fragility of the superconducting phase results in a high sensitivity to growth conditions, magnetic fields, and, as we show later, P . Although all crystals measured, more than 20, displayed $2.25 \leq T_{onset} \leq 2.5$ K in χ (Fig. 3 inset), a broad range of behavior was found in $\chi(T)$ with an incomplete Meissner effect observed in most crystals. This disparate behavior is demonstrated in Fig. 3 where the real and imaginary parts of the ac susceptibility χ' and χ'' , are plotted for two of the 3 crystals whose magnetic susceptibility was explored at dilution refrigerator temperatures. One crystal, sample s1, displays a very broad transition to a $\chi' = -1$ state at $T < 0.2$ K for ac excitation fields, H_{ac} , oriented along the c -axis. For H_{ac} oriented along the ab planes the diamagnetic signal remains incomplete for s1, approaching -0.75 at our lowest T , while the second sample, s2, displays only a small diamagnetic signal. The full Meissner state in s1 for $H_{ac} \parallel c$ is only apparent below 0.2 K despite a diamagnetism consistent with type I superconductivity at $T < 2.5$ K as demonstrated in Fig. 4. Here, similarly large anisotropies are apparent in the magnetic field, H , dependence of M , that faithfully reflect the crystalline structure. The dc H dependence of χ' and χ'' for s1 in the two field orientations are shown in Fig. 5 at a few T s. In Figs. 4 and 5 the small characteristic fields for the destruction of the Meissner state are apparent.

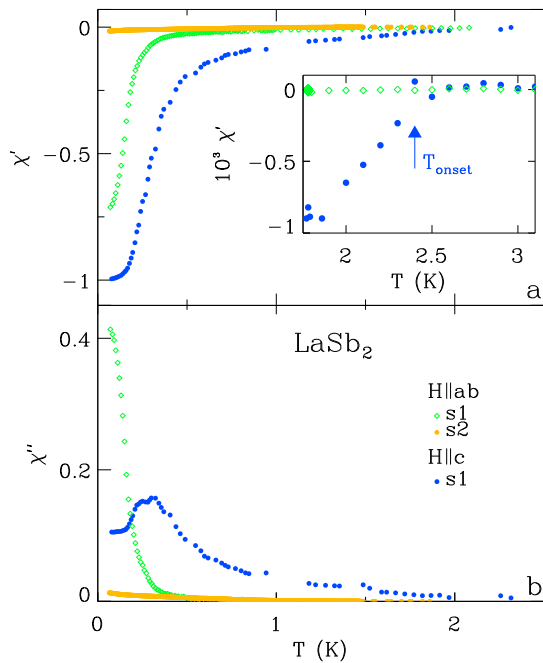


FIG. 3: Ambient pressure temperature dependent susceptibility. (a) Real part of the ac susceptibility, χ' , for excitation fields along the c-axis and in the ab plane vs. temperature, T , for two representative crystals, s1 and s2. Inset: detail near the onset of superconductivity, T_{onset} , as indicated by the arrow. The data for sample s1 in this frame have been previously presented in Ref.²⁵ which was published under license in Journal of Physics: Conference Series by IOP publishing Ltd. (b) The imaginary part of the ac susceptibility, χ'' for the same samples and field orientations as in frame (a). Symbols represent the same samples and orientations in both frames.

C. C. Hydrostatic Pressure

The application of pressure dramatically reduces the anisotropy and significantly sharpens the transition as we demonstrate in Figs. 6 and 7. Here we present the P , T , and H dependence of χ' for temperatures near the onset of superconductivity with the same field orientations as in Fig. 3. Although we have only followed χ' down to 1.78 K it is apparent that by 4.4 kbar the transition width has been reduced to ~ 0.1 K with $\chi' = -1$ at 1.8 K for $H_{ac} \parallel c$, while for $H_{ac} \parallel ab$, $\chi' < -0.75$. Increasing the pressure beyond 4.4 kbar leads to a reduction of T_{onset} without further change in the transition width apparent to 6.5 kbar. $\chi'(H)$ for the two H_{ac} orientations shown in Fig. 7 are much less anisotropic at these pressures as well, and a continuous reduction of H_c with P is apparent. In addition, we do not observe the sample-to-sample variability that was so apparent in the ambient pressure $\chi'(T)$.

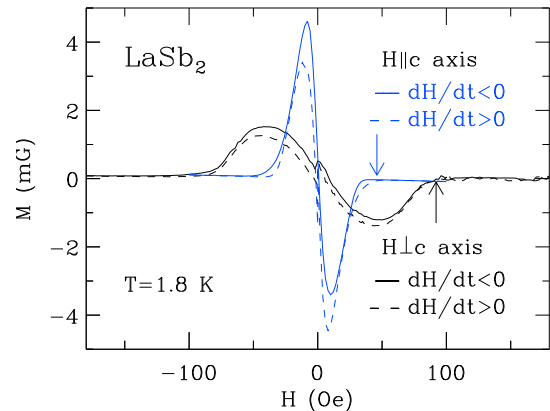


FIG. 4: Ambient pressure magnetization. Magnetization, M , at $T = 1.8$ K vs. H along the c-axis and ab planes. Arrows indicate critical fields for the destruction of superconductivity.

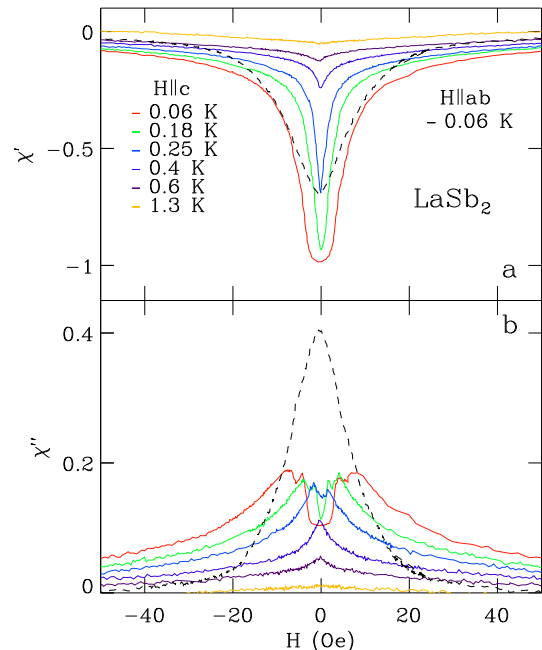


FIG. 5: Ambient pressure field dependent susceptibility. (a) Real part of the ac susceptibility, χ' , for sample s1 vs. magnetic field, H , at temperatures identified in the figure. Data shown at 60 mK for two orientations of the ac excitation field. (b) Imaginary part of the ac susceptibility, χ'' , for the same sample, temperatures, and field orientations as in frame (a).

D. D. Critical Field Anisotropy

We have explored the anisotropy of H_c by measuring $\rho(H)$ as a function of field orientation at 0.1 K in Fig. 8. We observe a factor of 4 difference in H_c as the crystal is rotated from an orientation where the ab planes are nearly parallel to H ($\theta = 0$), H_c^{\parallel} , until they are perpendicular to H ($\theta = 90^\circ$), H_c^{\perp} . For comparison we plot

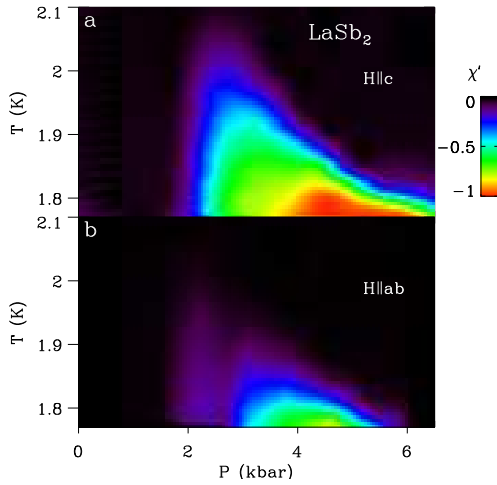


FIG. 6: Pressure and temperature dependence of the superconducting transition. Real part of the ac susceptibility, χ' , for magnetic fields, H , along the c -axis (a) and along the ab planes (b) vs. pressure, P , and temperature, T . These contour plots are produced by simple interpolation of measurements performed at 12 (11) different pressures in frame a (b). The data at 4.4 kbar in this figure have been previously presented in Ref.²⁵ which was published under license in Journal of Physics: Conference Series by IOP publishing Ltd.

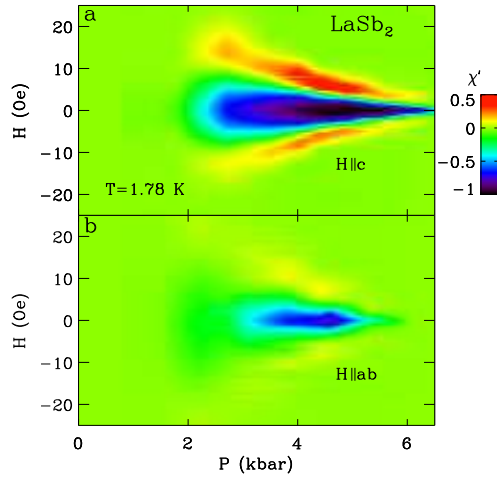


FIG. 7: Pressure and field dependence of the superconducting transition. Real part of the ac susceptibility, χ' , at 1.78 K vs. pressure, P , and magnetic field, H , along the c -axis (a) and along the ab planes (b). Data for increasing H shown in all frames. These contour plots are produced by simple interpolation of measurements performed at 12 (11) different pressures in frame a (b).

the 2D Tinkham formula³² prediction, solid line, having no adjustable parameters beyond fixing H_c^{\parallel} and H_c^{\perp} to match our data. The sharp cusp in the data as $\theta \rightarrow 0$ is considered a clear signature of 2D superconductivity. We note that H_c^{\parallel} is much smaller than the paramagnetic limit which has been exceeded in some layered materials^{3,4}.

Our measured H_c^{\parallel} is likely intrinsically limited by the long mean free path, ℓ , for the carriers and the related large diffusion constant³², as well as experimentally limited by the flatness of our crystals.

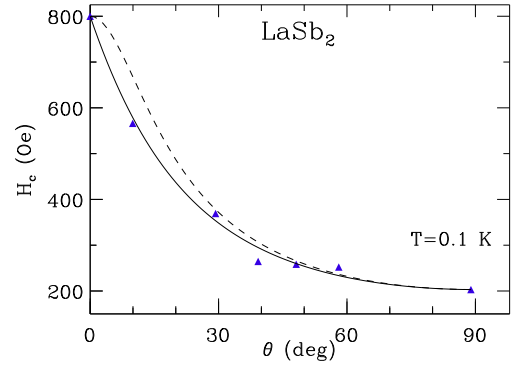


FIG. 8: Critical field angular dependence. Critical field for the suppression of superconductivity, H_c vs. angle, θ , from H parallel to the ab planes as measured in the resistivity at 0.1 K. Solid (dashed) line is a plot of the 2D (anisotropic 3D) Tinkham formula³².

In Fig. 9 we present the anisotropy in the critical fields at 1.78 K as a function of applied hydrostatic pressure, P , as determined by the real part of the ac magnetic susceptibility. In this experiment the crystal was nominally aligned ($\pm 10^\circ$) to the applied magnetic field as the sample space in the SQUID magnetometer did not allow for a careful sample rotation such as that carried out in Fig. 8 for the resistivity measurements. In Fig. 9 we quantify what is apparent in Fig. 7, a continuous reduction of the critical field anisotropy with P including isotropic behavior near 6 kbar.

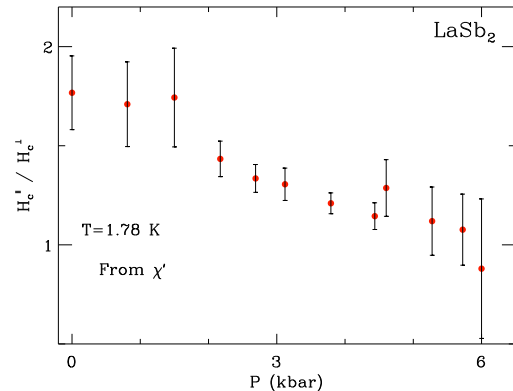


FIG. 9: Critical field anisotropy. Anisotropy of the critical field, H_c , for $H \parallel ab$ planes, H_c^{\parallel} , divided by that for $H \parallel c$ -axis, H_c^{\perp} , vs. pressure, P , as determined by the real part of the ac susceptibility at 1.78 K.

IV. IV. DISCUSSION AND CONCLUSIONS

Our data presented above reveal LaSb₂ to possess an exceedingly unusual SC phase characterized by large anisotropies for fields and currents parallel and perpendicular to the Sb planes. The SC transition is extraordinarily broad and, in the majority of samples, incomplete at $P = 0$. However, the SC transition is sharpened and the anisotropy reduced with application of moderate P . In addition, the SC state at $P = 0$ has an angular dependent H_c characteristic of a 2D superconductor along with features in ρ_c characteristic of quasiparticle tunneling between Sb planes. These observations lead us to conclude that LaSb₂ under ambient pressure conditions is undergoing two transitions: a planar superconducting transition initiating at T_{onset} and a secondary bulk transition below ~ 0.5 K associated with the emergence of coherent interlayer coupling. We believe that the interplane Josephson coupling of essentially 2D SC planes mediates the high pressure 3D phase. It follows that the sample-to-sample differences that we observed in the ambient pressure magnetization (see e.g. Fig. 3) is a manifestation of the sensitivity of our crystals due to the proximity of LaSb₂ to a fully 3D SC phase.

Estimates based upon our previous $\rho(T, H)$, Hall effect²⁶, and de Haas-van Alphen (dHvA)²⁴ measurements confirm our crystals have small carrier density, n , small carrier mass, m^* , and highly metallic in-plane transport that make anisotropic, type I (see Fig. 4), superconductivity sensible in LaSb₂. The Hall coefficient with $H \parallel c$ is indicative of $n = 2 \times 10^{20} \text{ cm}^{-3}$. The small n and low ρ_{ab} indicate highly conductive transport along the ab plane at low temperatures with an estimated Hall mobility of $2.7 \text{ m}^2/\text{Vs}$ and mean free path, ℓ , of $\sim 3.5 \mu\text{m}$ ²⁶. The reduction of the dHvA amplitudes with T is small so that m^* is only 0.2 times the bare electron mass²⁴. With these parameters, simple estimates³² of the London penetration depth, λ , and Pipard coherence length, ξ_0 , for currents in the ab plane give $\lambda \geq 0.15 \mu\text{m}$, dependent on the SC condensate fraction, and $\xi_0 = 1.6 \mu\text{m}$, much larger than in typical intermetallic compounds. The large ℓ puts our crystals in the clean limit with $\kappa = \lambda/\xi_0 < 1$ consistent with type I superconductivity and a small critical field, H_c . Type I superconductivity is rare in intermetallic compounds and its discovery here is a reflection of the extraordinarily long scattering times for currents in the ab planes^{26,28}.

There are several other mechanisms for these observations that we have considered. The first is the possibility that the SC state at $P = 0$ is restricted to the surfaces of the crystals and that a seemingly unrelated 3D SC state is induced by the application of P . The large Meissner fractions we observe in some of the samples and the continuous evolution of the SC state with P make this very unlikely. Second, we have considered the possibility that we are observing an anisotropic 3D SC state^{33–36} emanating from the 2D-like bands of LaSb₂²⁴. Anisotropic 3D superconductivity is consistent with the ratio of H_c^{\parallel}/H_c^c ,

but not the angular dependence in Fig. 8. In addition, it is difficult to explain the large anisotropy in ρ and $\chi'(T)$ in Figs. 1, 2 and Fig. 3 in such a scenario. Finally, we point out that the wide superconducting transition at ambient pressure is not likely caused by impurities or second phases in our crystals since our X-ray diffraction data are free from extraneous peaks, we deduce very long mean free paths for carrier transport along the ab planes, and because the application of moderate pressure is unlikely to suppress the effects of impurities or defects.

Thus, our data suggest that at low T LaSb₂ is best described as a set of Josephson coupled 2D planar superconductors. Interestingly, our observation of an extraordinarily wide, and often times incomplete SC transition at $P = 0$, along with the dramatic changes apparent with moderate P , indicate that the SC transition may be limited by phase and amplitude fluctuations of the SC order parameter. Emery and Kivelson have demonstrated that phase fluctuations are dominant when there is small phase stiffness¹⁸ and emphasize the role of small carrier density in amplifying the effects of phase fluctuations in high temperature cuprate superconductors. Experiments have revealed that the underdoped high T_c SC cuprates are indeed phase fluctuation limited¹⁹. In general, the importance of phase fluctuations can be determined by a comparison of T_c with the zero temperature phase stiffness, $V_0 \propto L/\lambda^2$, which gives the temperature at which phase order would disappear, T_θ^{max} ¹⁸. Here, L is the characteristic length scale which in quasi-2D superconductors is the larger of the spacing between SC layers or $\sqrt{\pi}\xi_\perp$, where ξ_\perp is the coherence length perpendicular to the ab planes. We point out that our estimated value for n for LaSb₂ from Hall effect measurements is only $\sim 2\%$ of a charge carrier per LaSb₂ formula unit which is small even when compared to the underdoped cuprates. As a result, when we make use of our estimated λ , and the assumption that $\xi_\perp < c/2 = 0.92 \text{ nm}$, the distance between Sb planes in LaSb₂, we find $T_\theta^{max} \leq 6.1$ times T_{onset} for superconductivity at ambient pressure (2.5 K). This value is comparable to that tabulated for the cuprates where T_θ^{max}/T_c ranges from 0.7 to 16¹⁸ and demonstrates that phase fluctuations may be important in determining the superconducting phase transition in LaSb₂.

One of the consequences of a phase limited transition is an extended temperature range where χ' is dominated by fluctuations at $T > T_c$. Ginzburg-Landau (GL) theory, applicable in proximity to T_c , predicts power-law dependencies for χ'/T in the reduced temperature, $t = T_c/(T - T_c)$ ³². To check for such power-laws in the T range over which the SC phase develops we have plotted $-\chi'/T$ as a function of t for s1, where we have used the maximum $\chi''(T)$ to define T_c , in Fig. 10. The lines in this figure represents the form expected in 2D, $\chi'/T \propto t$ and 3D where $\chi'/T \propto t^{0.5}$. The data at ambient pressure are well described by a power-law form over a decade in t with an exponent that approaches that of the GL 2D prediction. For larger t the data fall significantly below

this prediction displaying a behavior much more consistent with the 3D fluctuations. This cross-over to a 3D form is expected as ξ diverges at T_c . However, the large values of $-\chi'$ that we measure, for example at $t \sim 1$ we find $-\chi'/T \sim 0.1$, require $\xi_0 \sim 11 \mu\text{m}$, about 7 times the estimate based upon transport data. In contrast, the transitions at $P > 2$ kbar are not well described by a power-law in our range of t as is commonly the case when the SC state has a 3D character and the fluctuation dominated regime is restricted to much larger t .

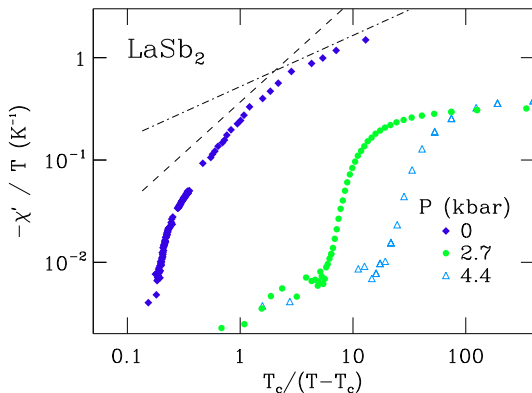


FIG. 10: Superconducting fluctuations. Negative of the ac magnetic susceptibility, χ' , divided by temperature, T , $-\chi'/T$ for $H \parallel$ to the c -axis vs. reduced temperature, $T_c/(T - T_c)$ with logarithmic axes. Sample s1 at $P = 0$ (blue diamonds) and for a second sample with $P = 2.7$ kbar (green bullets), and $P = 4.4$ kbar (blue triangles). The dashed-dotted line is a linear dependence and the dashed line is a square-root dependence representing the simplest model of 2 dimensional and 3 dimensional fluctuation limited superconductivity.

In order to sum up our data, we present a proposed pressure and temperature phase diagram that is consistent with our magnetization and resistivity measurements in Fig. 11. Since our ambient pressure magnetization data features some sample-to-sample variation, we chose to use sample s1, whose magnetic properties are demonstrated in Figs. 3, 5, and 10, as representative for the purposes of this phase diagram. This sample displays a large diamagnetic signal below 0.5 K and we have collected the most detailed data set for this crystal. Our proposed phase diagram features a 2D superconducting phase at the lowest temperatures and pressures, as well as an extended temperature and pressure range where 2D superconducting fluctuations are present. A 3D superconducting phase, along with attendant 3D superconducting fluctuations at slightly high temperatures, is stabilized by pressure. The 3D superconducting phase is expected to survive down to zero pressure only over a finite temperature range near T_c as ξ diverges. To demonstrate how this proposed phase diagram accurately describes LaSb_2 we have included some simple benchmarks as described in the figure caption. We have somewhat arbitrarily interpolated between the data points to draw the suggested boundaries between phases. As our data is

limited to temperatures above 1.75 K for pressures above ambient, there are regions that are not covered by our data so that the true T and P dependent behavior at pressures greater than ambient and $T < 1.75$ K has not been explored. Thus, the phase boundaries may be different from our interpolations in this region.

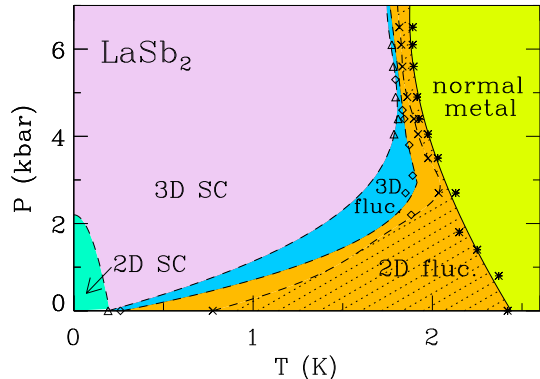


FIG. 11: Proposed Phase Diagram. Proposed temperature, T , and P , phase diagram. Symbols are onset of diamagnetism (*), 10% (x's) and 90% (triangles) of full Meissner for $H \parallel$ c -axis and 10% of full Meissner $H \parallel$ ab planes (diamonds). Lines are simple interpolations between the data points.

We conclude that at ambient pressure the anisotropic SC phase of LaSb_2 is fluctuation limited with fluctuations extending to T s an order of magnitude greater than T_c . The small carrier effective mass, long carrier mean-free-path, and small carrier density lead to large in-plane ξ_0 reducing the phase stiffness of the SC state. The application of pressure increases the Josephson coupling between the SC planes leading to a more traditional isotropic SC transition at the BCS T_c . Thus, our data suggest the existence of a quantum, $T = 0$, phase transition between 2D and 3D superconducting phases with P . In addition, LaSb_2 is a compelling candidate for investigating the pseudogap region where SC pairs are thought to form at T s above the phase ordering T , as in the underdoped cuprates, in a BCS superconductor without the complication of a competing ground state.

We are grateful to D. A. Browne and I. Vekhter for discussions. JFD, DPY, and JYC acknowledge support from the NSF through DMR0804376, DMR0449022, and DMR0756281. PWA acknowledges support from the DOE through DE-FG02-07ER46420.

- * ditusa@phys.lsu.edu
- ¹ F. R. Gamble, F. J. DiSalvo, R. A. Klemm, and T. H. Geballe, *Science* **168**, 568 (1970).
 - ² F. R. Gamble, J. H. Osiecki, M. Cais, and R. Pisharod, *Science* **174**, 493 (1971).
 - ³ D. E. Prober, M. R. Beasley, and R. E. Schwall, *Phys. Rev. B* **15**, 5245 (1977).
 - ⁴ D. E. Prober, R. E. Schwall, and M. R. Beasley, *Phys. Rev. B* **21**, 2717 (1980).
 - ⁵ S. Nagata, T. Aochi, T. Abe, S. Ebisu, T. Hagino, Y. Seki, and K. Tsutsumi, *J. Phys. Chem. Solids* **53**, 1259 (1992).
 - ⁶ D. Jérôme, A. J. Grant, and A. D. Yoffe, *Solid State Commun.* **9**, 2183 (1971).
 - ⁷ K. Aoi, R. Merservey, and P. M. Tedrow, *Phys. Rev. B* **9**, 875 (1974).
 - ⁸ Y. Liu, K. A. McGreer, B. Nease, D. B. Haviland, G. Martinez, J. W. Halley, and A. M. Goldman, *Phys. Rev. Lett.* **67**, 2068 (1991).
 - ⁹ T. Zhang, P. Cheng, W. J. Li, Y. J. Sun, G. Wang, X. G. Zhu, K. He, L. L. Wang, X. C. Ma, X. Chen, Y. Y. Wang, Y. Liu, H. Q. Lin, J. F. Jia, and Q. K. Xue, *Nat. Phys.* **6**, 104 (2010).
 - ¹⁰ S. Y. Qin, J. Kim, Q. Niu, and C-K. Shih, *Science* **324**, 1314 (2009).
 - ¹¹ J. Singleton and C. Mielke, *Contemp. Phys.* **43**, 63 (2002).
 - ¹² J. G. Bednorz and K. A. Muller, *Z. Phys. B - Condens. Mat.* **64**, 189 (1986).
 - ¹³ J. Nagamatsu, N. Nakagawam, T. Muranaka, Y. Zenitani, and J. Akimitsu, *Nature* **410**, 63 (2001).
 - ¹⁴ Y. Kamihara, H. Hiramatsu, M. Hirano, R. Kawamura, H. Yanagi, T. Kamiya, and H. Hosono, *J. Am. Chem. Soc.* **128**, 10012 (2006).
 - ¹⁵ Y. Kamihara, T. Watanabe, M. Hirano, and H. Hosono, *J. Am. Chem. Soc.* **130**, 3296 (2008).
 - ¹⁶ H. H. Wen, G. Mu, L. Fang, H. Yang, and X. Y. Zhu, *Europhys. Lett.* **82**, 17009 (2008).
 - ¹⁷ Z. A. Ren, W. Lu, J. Yang, W. Yi, X. L. Shen, Z. C. Li, G. C. Che, X. L. Dong, L. L. Sun, F. Zhou, and Z. X. Zhao, *Chin. Phys. Lett.* **25**, 2215 (2008).
 - ¹⁸ V. J. Emery and S. A. Kivelson, *Nature* **374**, 434 (1995).
 - ¹⁹ J. Corson, R. Mallozzi, J. Orenstein, J. N. Eckstein, and I. Bozovic, *Nature* **398**, 221 (1999).
 - ²⁰ A. G. Loeser, Z.-X. Shen, D. S. Dessau, D. S. Marshall, C. H. Park, P. Fournier, and A. Kapitulnik, *Science* **273**, 325 (1996).
 - ²¹ H. Ding, T. Yokoya, J. C. Campuzano, T. Takahashi, M. Randeria, M. R. Norman, T. Mochiku, K. Kadowaki, and J. Giapintzakis, *Nature* **382**, 51 (1996).
 - ²² Ch. Renner, B. Revaz, J. Y. Genoud, K. Kadowaki, and O. Fischer, *Phys. Rev. Lett.* **80**, 149 (1998).
 - ²³ S. L. Bud'ko, P. C. Canfield, C. H. Mielke, and A. H. Lacerda, *Phys. Rev. B* **57**, 13624 (1998).
 - ²⁴ R. G. Goodrich, D. Browne, R. Kurtz, D. P. Young, J. F. DiTusa, P. W. Adams, and D. Hall, *Phys. Rev. B* **69**, 125114 (2004).
 - ²⁵ LaSb₂ does not appear to support charge density wave order see J.F. DiTusa, V. Guritanu, S. Guo, D. P. Young, P. W. Adams, R. G. Goodrich, J. Y. Chan, and D. van der Marel., *J. Phys.: Conf. Ser.* **273**, 012151 (2011).
 - ²⁶ D. P. Young, R. G. Goodrich, J. F. DiTusa, S. Guo, P. W. Adams, J. Y. Chan, and D. Hall, *Appl. Phys. Lett.* **82**, 3713 (2003).
 - ²⁷ A. I. Acatrinei, D. Browne, Y. B. Losovyi, D. P. Young, M. Moldovan, J. Y. Chan, P. T. Sprunger, and R. L. Kurtz, *J. Phys. Cond. Matt.* **15**, L511 (2003).
 - ²⁸ See e.g. S. Yonezawa and Y. Maeno, *Phys. Rev. B* **72**, 180504R (2005).
 - ²⁹ N. Sato, T. Kinokiri, T. Komatsubara, and H. Harima, *Phys. Rev. B* **59**, 4714 (1999).
 - ³⁰ S. Guo, D. P. Young, R. T. Macaluso, D. A. Browne, N. L. Henderson, J. Y. Chan, L. L. Henry, and J. F. DiTusa, *Phys. Rev. B* **81**, 144423 (2010).
 - ³¹ P. Szabo, P. Samuely, J. Kacmarcik, A. G. M. Jansen, A. Briggs, A. Lafond, and A. Meerschaut, *Phys. Rev. Lett.* **86**, 5990 (2001).
 - ³² See e.g. M. Tinkham in "Introduction to Superconductivity" Kreiger (Malabar, FL) (1975).
 - ³³ W. E. Lawrence and S. Doniach in *Proc. 12th Int. Conf. Low Temp. Phys.*, Edited by E. Kanda (Academic, Kyoto, 1971).
 - ³⁴ C. S. L. Chun, G. G. Zheng, J. L. Vicent, and I. K. Schuller, *Phys. Rev. B* **29**, 4915 (1984).
 - ³⁵ I. Banerjee, Q. S. Yang, C. M. Falco, and I. K. Schuller, *Phys. Rev. B* **28**, 5037 (1983).
 - ³⁶ R. V. Coleman, G. K. Eiserman, S. J. Hillenius, A. T. Mitchell, and J. L. Vicent, *Phys. Rev. B* **27**, 125 (1983).